

# Designing robust chitosan-based hydrogels for stem cell nesting under oxidative stress

Zahra Olfat Noubari<sup>1</sup>, Asal Golchin<sup>1</sup>, Marziyeh Fathi<sup>1\*</sup>, Ailar Nakhband<sup>2,1\*</sup>

<sup>1</sup>Research Center for Pharmaceutical Nanotechnology, Biomedicine Institute, Tabriz University of Medical Sciences, Tabriz, Iran

<sup>2</sup>Research Center of Psychiatry and Behavioral Sciences, Tabriz University of Medical Sciences, Tabriz, Iran

## Article Info



### Article Type:

Original Article

### Article History:

Received: 12 May 2021

Revised: 16 June 2021

Accepted: 20 June 2021

ePublished: 16 Oct. 2021

### Keywords:

Hydrogel  
 Chitosan  
 Mesenchymal stem cells  
 Oxidative stress  
 Gene expression  
 Tissue engineering

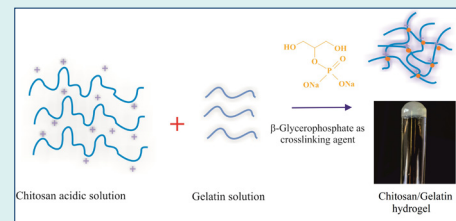
## Abstract

**Introduction:** Hydrogels are unique candidates for a wide range of biomedical applications including drug delivery and tissue engineering. The present investigation was designed to consider the impact of chitosan-based hydrogels as a scaffold on the proliferation of human bone marrow mesenchymal stem cells (hBM-MSCs) besides neutralization of oxidative stress in hBM-MSCs.

**Methods:** Chitosan (CS) and CS-gelatin hydrogels were fabricated through ionic crosslinking using  $\beta$ -glycerophosphate. The hBM-MSCs were cultured on the prepared matrices and their proliferation was evaluated using DAPI staining and MTT assay. Furthermore, the effect of hydrogels on oxidative stress was assessed by measuring the expression of NQO1, Nrf2, and HO-1 genes using real-time PCR.

**Results:** The developed hydrogels indicated a porous structure with high water content. The toxicity studies showed that the prepared hydrogels have a high biocompatibility/cytocompatibility. The expression of intracellular antioxidant genes was studied to ensure that stress is not imposed by the scaffold on the nested cells. The results showed that Nrf2 as a super transcription factor of antioxidant genes and its downstream antioxidant gene, NQO1 were downregulated. Unexpectedly, the upregulation of HO-1 was detected in the current study.

**Conclusion:** The prepared CS-based hydrogels with desired properties including porous structure, high swelling ability, and cytocompatibility did not show oxidative stress for the nesting of stem cells. Therefore, they could be attractive scaffolds to support stem cells for successful tissue engineering purposes.



## Introduction

Mesenchymal stem cells (MSCs) have gained growing attention as an efficient therapeutic approach for various chronic diseases. These cells can be isolated from various sources such as bone marrow, skeletal muscle, adipose tissue, amniotic fluid, fetal blood, synovium, dental pulp, and umbilical cord.<sup>1</sup> It is well documented that extracellular matrix (ECM) is vitally required to surround and support the cells structurally. Moreover, ECM plays an important role in regulating the cell function by providing biochemical and biomechanical signals.<sup>2</sup> Evidence supports that the interaction with microenvironment affects the function of the injected stem cells in tissue engineering approaches.<sup>3</sup> Engineered biomaterials provide a suitable platform to best mimic the microenvironment of the MSCs and to improve cell function and viability.<sup>3,4</sup>

Hydrogels are considered as one of the best candidates for supporting MSC growth and differentiation.<sup>3,5</sup> It is well established that hydrogels are water-swollen networks that facilitate cell attachment, proliferation, and biomolecule transportation.<sup>6-9</sup> Moreover, injectable hydrogels demonstrated unique properties for drug delivery and tissue engineering applications. They can encapsulate cells, or therapeutic substances including drugs, proteins, and even genes under a controlled manner. The most unique properties of hydrogels include hydrophilic and environment-friendly structure, ability to form a solid gel, and sensitivity to temperature and pH. Hydrogels are biocompatible biomaterials and have a similar structure to ECM with low protein absorption due to low surface tension. These properties make hydrogels efficient biomaterials for various medical applications including



\*Corresponding authors: Marziyeh Fathi, [fathi.marziyeh@yahoo.com](mailto:fathi.marziyeh@yahoo.com); [fathim@tbzmed.ac.ir](mailto:fathim@tbzmed.ac.ir); Ailar Nakhband, [ailarnakhband@yahoo.com](mailto:ailarnakhband@yahoo.com)



© 2022 The Author(s). This work is published by BioImpacts as an open access article distributed under the terms of the Creative Commons Attribution License (<http://creativecommons.org/licenses/by-nc/4.0/>). Non-commercial uses of the work are permitted, provided the original work is properly cited.

tissue engineering, controlled release of therapeutic agents (proteins, drugs, genes), contact lens fabrications, and wound healing.<sup>10-15</sup>

Chitosan (CS) as the most abundant biocompatible, biodegradable, and mucoadhesive biopolymer can be utilized for the preparation of thermosensitive injectable hydrogels using  $\beta$ -glycerophosphate ( $\beta$ -GP) as an ionic crosslinking agent in physiological conditions.<sup>16-18</sup> The low mechanical strength of CS-based hydrogels has restricted their biomedical applications. The combination of CS with gelatin not only result in the improvement of mechanical properties of CS but also provides a suitable scaffold for cell survival in tissue engineering due to the similar structure to the collagen and mimicking the ECM.<sup>19</sup>

Regarding regenerative medicine, the damage of individual cells and host cells due to reactive oxygen species (ROS)-induced oxidative stress is a major obstacle to successful tissue engineering and regeneration. Decreased oxidative stress leads to MSCs' promoted proliferation besides DNA stability.<sup>20,21</sup> Despite high contents of glutathione and an active antioxidant system in MSCs, they endure ROS production as they replicate. Elevated levels of ROS lead to a decreased cell differentiation though in adipose tissue, it is the opposite.<sup>21</sup> Therefore, we aimed to design a CS/gelatin hydrogel system for promoting the therapeutic potential of stem cells with a focus on overcoming oxidative stress.

## Materials and Methods

### Materials

CS (medium molecular weight with a deacetylation degree of (75%–85%)), gelatin (porcine skin),  $\beta$ -glycerophosphate (GP) disodium salt hydrate, and methyl thiazolyl tetrazolium (MTT) reagent were provided from Sigma-Aldrich Corp. (St. Louis, MO, United States). MSCs were obtained from the National Institute of Genetic Resources (Tehran, Iran). Cell culture flasks and plates and all disposable equipments were bought from IWAKI (CITY, Japan). Low Glucose DMEM medium, fetal bovine serum (FBS), and trypsin-EDTA (0.02–0.05%) were bought from Gibco (Paisley, UK). Ethanol, HCL, chloroform, and isopropanol were purchased from Merck (Kenilworth, United States). Complementary DNA synthesis kit was bought from Fermentas (Waltham, Canada). All the primers were provided by MWG Biotech (Ebersberg, Germany).

### Preparation of temperature-sensitive CS and CS/gelatin hydrogels

To fabricate hydrogels, 0.2 g of CS powder with a medium molecular weight was autoclaved at 121°C for 20 minutes. Afterward, 0.1M hydrochloric acid was filtered by a 0.22  $\mu$ m syringe filter and added to the sterile CS powder to dissolve it. Then 1 g of GP was dissolved in distilled water. The GP solution was filtered using a 0.22  $\mu$ m syringe filter. For the preparation of CS hydrogel (A), the GP solution

was added dropwise to the CS solution and mixed in an ice bath to prevent the gelation. After mixing for 15 minutes, the pH of each mixture was evaluated and set to be 7.4. The obtained solutions were placed in an incubator of 5% CO<sub>2</sub> and 37°C for hydrogel formation. Moreover, for the preparation of CS-gelatin hydrogels (B, C), the sterile gelatin solution (4% w/v) was prepared using autoclaved gelatin powder with sterile distilled water by mixing 0.4 g gelatin in 10 mL distilled water.<sup>22</sup> Hydrogels B and C were prepared in the same way by adding gelatin to the CS solution. Table 1 indicates the composition of the prepared hydrogels.

### Structural analysis by FT-IR and morphology study of hydrogels using scanning electron microscopy

The chemical structure of the hydrogels was studied through Fourier transform infrared (FT-IR) spectroscopy. KBr tablets were used for FT-IR analysis. Scanning electron microscopy (SEM, Zeiss DSM-960A, Germany) was used to investigate the morphology and structural features of the hydrogels.

### Investigation of swelling behavior of hydrogels

To calculate the swelling ratio of hydrogels, the hydrogel samples were freeze-dried and incubated at 37°C in phosphate-buffered saline (PBS) solution and their weight was measured at different time intervals. The swelling percentage was calculated by the following formula (1):

$$\text{Swelling ratio (\%)} = \left( \frac{w_t - w_0}{w_0} \right) \times 100 \quad (1)$$

Where  $w_0$  is the weight of dried gel and  $w_t$  is the weight of the swollen hydrogel.

### ExVivo red blood cell hemolysis assay

Ex vivo red blood cell hemolysis assay was performed to consider the hemolytic potential of the hydrogel in human whole blood. To evaluate the effect of hydrogels on hemolysis, 0.5 mL of hydrogels were added to the tubes. Afterward, 0.5 mL of blood was poured into each falcon plus 3 mL of PBS and incubated at 37°C for one hour with shaking. Afterward, the tubes were subjected to centrifugation at 160 g for 12 minutes. After the separation of the supernatant, its light absorption percentage was measured by a spectrophotometer at 545 nm. PBS was employed as the negative control (0% lysis) and distilled

Table 1. Composition of prepared hydrogels

Hydrogel	Composition of ingredients
A	1 mL chitosan 2% + 200 $\mu$ L glycerophosphate 40%
B	600 $\mu$ L chitosan 2% + 200 $\mu$ L glycerophosphate 40% + 400 $\mu$ L gelatin 4%
C	800 $\mu$ L chitosan 2% + 200 $\mu$ L glycerophosphate 40% + 200 $\mu$ L gelatin 4%

water was used as the positive control (100% lysis).<sup>23</sup>

The percentage of hemolysis was calculated by the following formula (2):

$$\text{Hemolysis (\%)} = \frac{(OD_{\text{sample}} - OD_{\text{negative}})}{(OD_{\text{positive}} - OD_{\text{negative}})} \times 100 \quad (2)$$

### Biocompatibility and cell toxicity assay

To assess the cytotoxicity of hydrogels, an MTT assay was implemented according to the literature.<sup>24,25</sup> hBM-MSCs were cultured and incubated in a humidified incubator with 95% air and 5% CO<sub>2</sub> at 37°C. The cell culture medium was composed of low glucose DMEM supplemented with 10% (v/v) fetal bovine serum and antibiotics [penicillin G (100 U/mL) and streptomycin (100 µg/mL)]. Cytotoxicity of CS-based hydrogels on MSCs was evaluated using the MTT assay via extraction based on ISO 10993-5 guidelines. To this end, hydrogels' solutions were developed as mentioned above and added to 6-well culture plates (1 mL/well) and incubated at 37°C to form the gels. Then the complete medium (5 mL/well) was added to the formed hydrogels and incubated at 37°C for 24 hours. The obtained leachates were strilled through filtering with a 0.22 µm syringe filter. To perform the MTT test, MSCs were cultured in 96-well plates at their exponential phase. After 24 hours of cultivation, the cells were exposed to the whole extracted solution of the hydrogel. A normal complete culture medium was added to the negative control sample and 5% DMSO was added to provide positive control. To prepare the leachates, 5 mL complete medium was added to 1 mL of the formed hydrogels for 24 hours at 37°C. They were filtrated through a 0.22 µm syringe filter.

After the incubation period for 24 and 48 hours, the culture medium was replaced with a solution containing 50 µL MTT solution (2 mg/mL in PBS) and 150 µL of fresh medium. After 4 hours of incubation at 37°C, the MTT solution was removed and substituted with 200 µL of DMSO and 25 µL of Sorenson buffer (0.1 M glycine, 0.1 M NaCl, pH 10.5). Through this procedure, metabolically active cells produced formazan crystals which were dissolved in DMSO and the absorbance was measured at 570 nm via a spectrophotometric plate reader, ELx 800 (Biotek, CA, USA).

### DAPI staining for detection of apoptotic cells

The DAPI staining was conducted according to a

previously published report to detect the possible incidence of nucleus condensation in cells injected into hydrogels.<sup>26</sup> Briefly, 48 hours after injection of treated cells into the hydrogels, the cells were fixed with the freshly prepared ice-cold paraformaldehyde (4%) and exposed to 0.1% Triton X-100 in PBS for 5 minutes and permeabilized. Subsequently, cells were stained with DAPI (1 µg/mL in PBS) for 5 minutes in the dark. After removal of surplus stain, the cells were washed (3×) using 0.1% Triton X-100 in PBS. The image acquisition was achieved by Olympus IX81 invert fluorescence microscope equipped with an Olympus DP70 camera.

### Real-time PCR studies

Hydrogels' impact on oxidative stress in hBM-MSCs was studied via a quantitative iQ5 real-time PCR detection system (Bio-Rad Laboratories Inc., Hercules, USA). To this end, the expression levels of oxidative stress-related genes including nuclear factor erythroid 2-related factor 2 (Nrf2), heme oxygenase 1 (HO-1), NAD(P)H (Nicotinamide Adenine Dinucleotide plus Hydrogen), and quinone oxidoreductase 1 (NQO1) were investigated. Total RNAs from the control and hBM-MCSs cultured on the hydrogel were isolated with the RNeasy Mini Kit (Qiagen, Hilden, Germany) based on the company's protocol. The integrity of the isolated RNA was assessed by agarose gel electrophoresis while the purity and concentration of RNAs were tested by optical density measurement (A260/A280 ratio) with a nanodrop device (ND 1000, USA). Subsequently, 1 µg of the isolated RNA sample was used to develop complementary DNA (cDNA). Primers were designed using published gene bank sequences via Oligo 7.56 (Molecular Biology Insights, Inc., USA) as shown in Table 2. Each reaction composition included 1 µL cDNA, 1 µL primer (100 nM each primer), 12.5 µL 2× SYBR Green PCR Master Mix (Applied Biosystems, Foster City, USA), and 10.5 µL RNase/DNase free water. Thermal cycling settings were as follows: 1 cycle at 94°C for 10 minutes, 40 cycles at 95°C for 15 seconds, 60–63°C for 30 seconds, and 72°C for 25 seconds. Results were interpreted by the Pfaff method and the CT values were normalized to the expression proportion of β-actin as a housekeeping gene. All reactions were implemented in triplicate and each assay included negative control.

### Statistical analysis

One-way analysis of variance (ANOVA) followed by a

**Table 2.** The sequences of the used primers

Gene	Sequence	Size (bp)	Tm (°C)	Ref.
Nrf2	Forward GAGACAGGTGAATTTCTCCCAAT	120	54	20
	Reverse TTTGGGAATGTGGGCAAC			
HO-1	Forward ACGGCTTCAAGCTGGTGATG	118	59	20
	Reverse TGCACTCTTCTGGGAAGTAG			
NQO1	Forward ATGTATGACAAAGGACCTTCC	124	60	20
	Reverse TCCCTTGCAAGAGTACATGG			

Tukey post hoc test was performed to study the average differences between data (SPSS 13.0 software; SPSS Inc., Chicago, IL, USA). All results were presented as mean  $\pm$  SD. A *P* value less than 0.05 was defined as statistically significant.

## Results

### Evaluation of hydrogel structure

In the FT-IR spectra of hydrogels (Fig. 1), CS-related functional groups exist at different wavelengths. The broad peak in the spectrum of hydrogel (A) exists at  $1070\text{ cm}^{-1}$  that is related to the tensile vibrations of C-O. The peaks in  $1642\text{ cm}^{-1}$  and  $1529\text{ cm}^{-1}$  are related to the tensile vibration of the CS amide group and bending vibration of the CS amine group, respectively. The N-H CS bending vibration of the amide II has appeared at  $1461\text{ cm}^{-1}$ . The broad peaks of the hydroxyl and CS amine groups can be seen at  $3000\text{--}3500\text{ cm}^{-1}$ . The peak in  $972\text{ cm}^{-1}$  belongs to the GP group. There was no obvious difference in FT-IR spectra between hydrogel sols and gels (Fig. 1). The spectra of hydrogels B and C, which contain gelatin are similar to the spectrum of hydrogel A due to the overlapping of their functional group peaks and they only indicated some wider peaks compared to hydrogel A.

The microstructure of hydrogels A, B, C was evaluated by SEM (Fig. 2). According to the SEM images, hydrogels indicated interconnected porous structures with different sizes. The porous structure of the hydrogels allows the high permeability of the hydrogels, resulting in the loading of drugs and cells into the hydrogel matrix, making them suitable for drug release and tissue engineering. Gelatin affected the microstructure of hydrogels and hydrogel with the looser structure was obtained with gelatin incorporation.

The swelling property of hydrogel has an important effect on their biomedical applications. The swelling

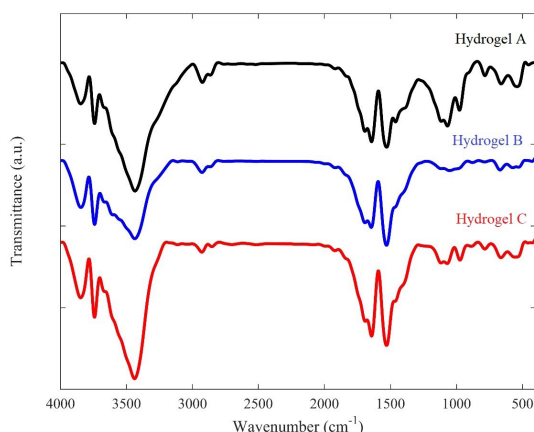


**Fig. 1.** FT-IR spectra of the prepared hydrogels (A, B, and C). Hydrogel A: 1 mL Chitosan 2% + 200  $\mu\text{L}$  Glycerophosphate 40%; Hydrogel B: 600  $\mu\text{L}$  Chitosan 2% + 200  $\mu\text{L}$  Glycerophosphate 40% + 400  $\mu\text{L}$  Gelatin 4%; hydrogel C: 800  $\mu\text{L}$  Chitosan 2% + 200  $\mu\text{L}$  Glycerophosphate 40% + 200  $\mu\text{L}$  gelatin 4%.

ratio of hydrogels was evaluated by soaking them in PBS solution (Fig. 3). Hydrogels B and C showed a more swelling ratio compared to hydrogel A which indicated that gelatin causes more water uptake in the hydrogel matrix.

A hemolysis test was performed after three hours of incubation. The supernatants were clear compared to the negative control. In comparison to the control group, the calculation of adsorption percentage did not show any significant difference in hydrogel samples (Fig. 4).

### Cell biocompatibility of the scaffold

Toxicity of hydrogels and hBM-MSCs viability were assessed via MTT colorimetric assay (Fig. 5). No significant toxicity was observed on mesenchymal cells injected in type A, B, and C hydrogels after 24 hours. It seems that the eluted materials from hydrogel are interfering with absorption, hence the chart had an ascending trend. Based on the cytotoxicity evaluation, the results presented that no significant in vitro toxicity was observed compared with untreated cells ( $P < 0.001$ ). However, it seems that gelatin in hydrogel formulation may result in some toxicity which can be attributed to more release of free  $\beta$ -GP molecules

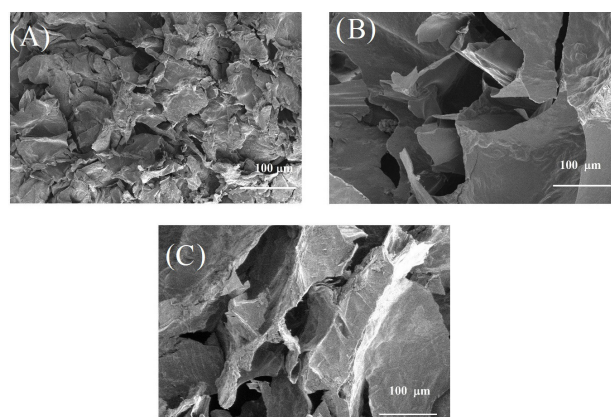


**Fig. 2.** SEM images of the fabricated hydrogels (A, B, and C). (A) Hydrogel A: 1 mL Chitosan 2% + 200  $\mu\text{L}$  Glycerophosphate 40%; (B) hydrogel B: 600  $\mu\text{L}$  Chitosan 2% + 200  $\mu\text{L}$  Glycerophosphate 40% + 400  $\mu\text{L}$  Gelatin 4%; (C) Hydrogel C: 800  $\mu\text{L}$  Chitosan 2% + 200  $\mu\text{L}$  Glycerophosphate 40% + 200  $\mu\text{L}$  Gelatin 4%.

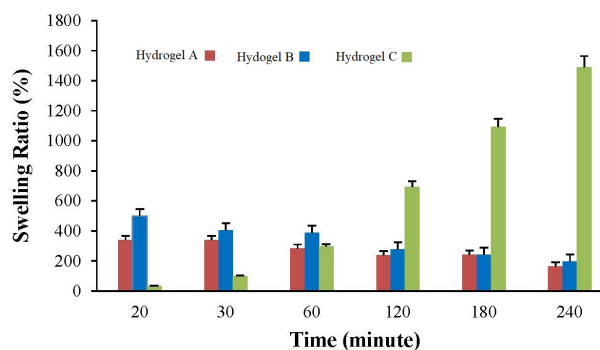


**Fig. 3.** Swelling behavior of hydrogels (A, B, and C) at different time intervals.

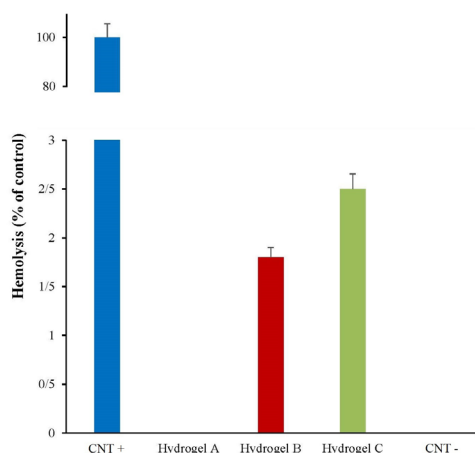


**Fig. 4.** Percentage of blood hemolysis in prepared hydrogels (A, B, and C). Distilled water and PBS were used as positive and negative controls (CNT), respectively.

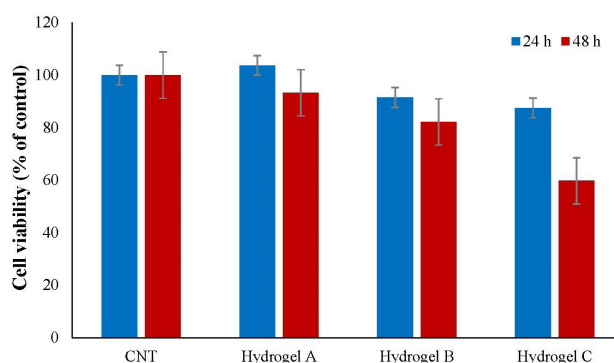


**Fig. 5.** The hBM-MSCs viability after 24 and 48 hours culturing in type A hydrogel (chitosan-based hydrogel), type B hydrogel (400  $\mu$ L gelatin), type C hydrogel (200  $\mu$ L of gelatin), and CNT (control mesenchymal cells in culture medium). Data represent mean  $\pm$  standard deviation ( $n=3$ ). No significant toxicity was observed in comparison with untreated cells ( $P > 0.05$ ).

due to the less crosslinked network. Therefore hydrogels A would be selected to be the best.

#### DAPI staining

The viability of injected cells in the hydrogel was assessed with DAPI staining. The results demonstrated that cells

injected to hydrogels did not show any morphological changes compared to the control cells (Fig. 6). Moreover, no apoptosis and nuclear fragmentation were observed in the cells cultured on the scaffold compared to the control samples. However, not much growth was observed in the cells injected in the hydrogel, but the viability of the cells in hydrogel A was observed and confirmed.

#### Intracellular antioxidants gene expression

The effect of hydrogel on intracellular oxidative stress was determined by examining the mRNA expression of some key intracellular antioxidants enzymes. Nrf2 is a transcription activator that attaches to the antioxidant response elements in the promoter regions of target antioxidant genes and is critical for the harmonized up-regulation of genes in response to oxidative stress.<sup>20</sup> As shown in Fig. 7, a decreased profile level of Nrf2 was detected in the cells nested at the CS scaffold ( $P=0.003$ ). This finding indicates that the designed hydrogel does not induce oxidative stress on the established cells. It was expected that Nrf2 downstream signaling genes including HO-1 and NQO1 be down-regulated, but surprisingly HO-1 upregulation was observed in nested cells.

#### Discussion

Applying hydrogels for therapeutic applications began in the 1960s when Lim and Wichterle synthesized the poly(hydroxyethyl methacrylate) bridge.<sup>31</sup> As water is the largest component of the human body and a hydrogel can have a high water absorption, the use of hydrogels has been potentially considered in biomedicine in areas such as tissue engineering, drug delivery, cell therapy, and anesthetic delivery. Hydrogels, compared to other types of biological materials, have the advantages of increasing biological compatibility, biodegradability, adjustability, good mechanical strength, and porous structure. However, due to the low mechanical strength and brittle nature of hydrogels, the possibility of using hydrogels is still limited; thus, the studies which are concerned with their effective types including CS-based hydrogels are still in progress only due to the high biocompatibility of such gels.<sup>10,11,32</sup> Stem cells such as MSCs are regarded as useful cells

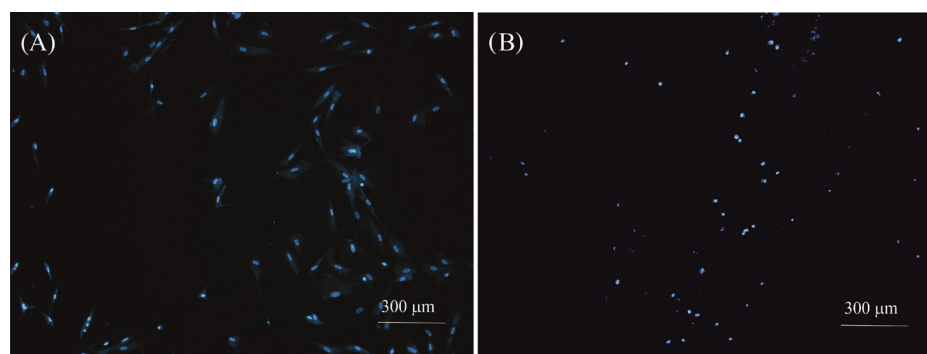


**Fig. 6.** DAPI-stained cell nucleus images with 4X magnification. (A) Control cells and (B) Cells were cultured on a hydrogel A scaffold. Apoptosis or nuclear fragmentation were not observed in cells injected to hydrogel compared to the control sample.

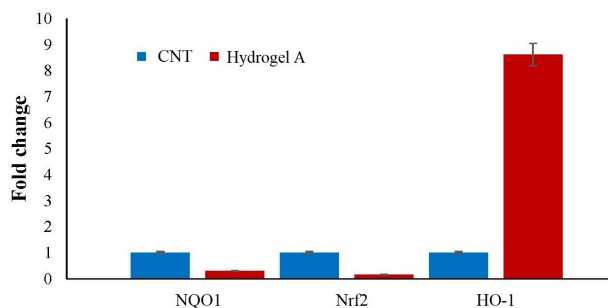


**Fig. 7.** Expression of antioxidant genes in MSCs nested on hydrogel A scaffold. Nrf2 and its downstream antioxidant gene, NQO1 were downregulated ( $P=0.003$ ,  $P=0.0013$  respectively). This finding indicates that the designed hydrogel does not induce oxidative stress on the established cells. Unexpectedly, the upregulation of HO-1 was detected as well which may be due to the natural need of MSCs for HO-1 activity to growth and differentiation.

owing to their potential immunomodulatory properties in alleviating diseases caused by inflammatory responses of immune cells in some diseases such as type 1 diabetes, rheumatoid arthritis, and multiple sclerosis.<sup>33-36</sup> CS and CS/gelatin hydrogels were synthesized and characterized in the current study.

In the FT-IR spectra (Fig. 1), the characteristic peaks of CS, gelatin, and  $\beta$ -GP confirmed the fabrication of hydrogel. According to the SEM images (Fig. 2), all hydrogels have a porous structure, however, the addition of gelatin caused the increase of pores size. It is assumed that the presence of gelatin (Figs. 2B and C) caused the decrease of electrostatic reaction of CS functional groups in the presence of  $\beta$ -GP as an ionic crosslinking agent that resulted in the larger pores. This was confirmed via swelling data (Fig. 3), as the hydrogels B and C have a relatively higher swelling ratio compared to hydrogel A.

The cytotoxicity assays via hemolysis (Fig. 4) and MTT (Fig. 5) demonstrated the compatibility of the developed hydrogels. CS/gelatin and GP as non-toxic materials are accepted for biomedical applications that resulted in non-toxic hydrogels.

In the present study, the effect of the CS-based hydrogels on the proliferation and redox state of hBM-MSCs was evaluated. Nrf2 gene was studied to identify the pathway of resistance to oxidative stress caused by the hydrogel. The results showed that there was no significant increase in Nrf2 gene expression. To recognize the exact pathway of resistance to oxidative stress by stem cells, another gene called NQO-1, antioxidant genes involved in the cellular oxidative stress pathway, was studied. It can be interpreted that culturing cells in hydrogels reduces oxidative stress-induced gene expression. Since the NQO-1 gene possesses a key role in the pathway of cellular oxidative stress, therefore we can demand that hydrogels have a protective effect on stem cells against oxidative stress. Another gene that was examined in this study was Nrf2. Culturing cells in hydrogels reduces the Nrf2 gene expression level. Because of the importance of the Nrf2 gene in the pathway of cellular oxidative stress,<sup>29,30</sup> it can

be concluded that hydrogel has a protective effect on stem cells against oxidative stress. In a study carried out by Tang et al, it was concluded that one of the causes of cell death was oxidative stress that was induced by apoptosis and caspases. By inhibiting caspase, catalase degradation continued and ROS increased which led to cell death. They found that this cell death was caused by autophagy.<sup>5</sup>

The results of the recent study showed that Nrf2 has been developed as a major regulator of oxidant resistance and has been used in a range of toxicities and chronic diseases associated with oxidative stress. Nrf2 is activated by the evolutionarily conserved Keap1-dependent mechanism of depression signaling.<sup>14</sup> While Nrf2 is inhibited under basal conditions by protease cleavage and keap1-controlled ubiquitination, it is activated by oxidants and ultrafilters by modulating the cysteine thiols of Keap1 and Nrf2. Activated Nrf2 mediates the expression of the induction of each of the signaling enzymes and proteins for metabolic regulation and antioxidant defense and oxidant signaling; therefore, it affects the physiology and pathobiology of the oxidant.<sup>14</sup> Nrf2 participates in the control of several programming roles, such as inhibitory signaling autophagy, apoptosis, mitochondrial biogenesis, and stem cell regulation. This is mainly done by regulating oxidant levels and oxidant signaling.<sup>37</sup>

The present study showed that culturing cells in hydrogels increases the expression of the HO-1 gene. According to the literature, upregulation of HO-1 expression levels and elevated activity of HO-1 are needed for MSCs growing and differentiation.<sup>27</sup> In addition, MSCs increase the expression of HO-1 due to their anti-inflammatory activity.<sup>28</sup> Therefore, MSCs may always need high levels of HO-1 naturally for normal activity, and the upregulated profile is not related to the stressed condition.

## Conclusion

The CS and CS/gelatin hydrogels were fabricated and characterized as a scaffold for the proliferation of hBM-MSCs. The prepared hydrogels indicated the porous structure with the high swelling ability and cytocompatibility properties. The results of gene expression evaluation in MSCs nested on prepared hydrogel indicated that the Nrf2 and its downstream antioxidant gene, NQO1 were downregulated which confirms no induction caused by oxidative stress on the established cells. On the other hand, the upregulation of HO-1 was detected as well which may be due to the natural need of MSCs to HO-1 activity for growth and differentiation. Hence, for the robust nesting of stem cells in oxidative stress and hypoxic injured tissues, the CS-based hydrogel could be an attractive candidate to support stem cells for successful cell therapies.

## Acknowledgments

The authors would like to acknowledge RCPN for financial and technical support.

## Research Highlights

### What is the current knowledge?

- ✓ The CS and CS/gelatin hydrogels have been fabricated and evaluated as a scaffold for the proliferation of hBM-MSCs.
- ✓ Oxidative stress is a major issue in successful tissue engineering.

### What is new here?

- ✓ The effect of prepared hydrogels on oxidative stress was assessed by investigating the expression of NQO1, Nrf2, and HO-1 genes using real-time PCR.
- ✓ The cellular and molecular evaluation demonstrated no oxidative stress induced by the prepared CS-based hydrogels.
- ✓ The CS-based hydrogel could be considered as an attractive candidate for supporting stem cells for successful cell therapies.

### Funding sources

This work was supported by the Research Center for Pharmaceutical Nanotechnology (RCPN) at Tabriz University of Medical Sciences.

### Ethical statement

There is none to be disclosed.

### Competing interests

The authors declare that there is no conflict of interests.

### Authors' contribution

This work was carried out in collaboration with all authors. MF and AN designed the study. ZON did the experiments, collected the data, analyzed the data, and wrote the manuscript. AG collaborated in cellular experiments. MF and AN edited the manuscript. All authors read and approved the final manuscript.

### References

1. Hosseiniyan Khatibi SM, Kheyrolahzadeh K, Barzegari A, Rahbar Saadat Y, Zununi Vahed S. Medicinal signaling cells: A potential antimicrobial drug store. *J Cell Physiol* **2020**; 236: 3257-74. <https://doi.org/10.1002/jcp.29728>
2. Barzegari A, Gueguen V, Omid Y, Ostadrahimi A, Nouri M, Pavon-Djavid G. The role of Hippo signaling pathway and mechanotransduction in tuning embryoid body formation and differentiation. *J Cell Physiol* **2020**; 235: 5072-83. <https://doi.org/10.1002/jcp.29455>
3. Barzegari A, Omid Y, Ostadrahimi A, Gueguen V, Meddahi-Pellé A, Nouri M, *et al.* The role of Piezo proteins and cellular mechanosensing in tuning the fate of transplanted stem cells. *Cell Tissue Res* **2020**; 381: 1-12. <https://doi.org/10.1007/s00441-020-03191-z>
4. Khoe S, Kardani M. Hydrogels as Controlled Drug Delivery Carriers. *Polymerization, Quarterly* **2013**; 2: 16-27.
5. Tang X-Q, Feng J-Q, Chen J, Chen P-X, Zhi J-L, Cui Y, *et al.* Protection of oxidative preconditioning against apoptosis induced by H<sub>2</sub>O<sub>2</sub> in PC12 cells: mechanisms via MMP, ROS, and Bcl-2. *Brain Res J* **2005**; 1057: 57-64. <https://doi.org/10.1016/j.brainres.2005.07.072>
6. Radhakrishnan J, Krishnan UM, Sethuraman S. Hydrogel based injectable scaffolds for cardiac tissue regeneration. *Biotechnol Adv* **2014**; 32: 449-61. <https://doi.org/10.1016/j.biotechadv.2013.12.010>
7. Thambi T, Li Y, Lee DS. Injectable hydrogels for sustained release of therapeutic agents. *J Control Release* **2017**; 267: 57-66. <https://doi.org/10.1016/j.jconrel.2017.08.006>
8. Hoffman AS. Hydrogels for biomedical applications. *Adv Drug Deliv Rev* **2012**; 64: 18-23. <https://doi.org/10.1016/j.addr.2012.09.010>
9. Akhtar MF, Hanif M, Ranjha NM. Methods of synthesis of hydrogels... A review. *Saudi Pharm J* **2016**; 24: 554-9. <https://doi.org/10.1016/j.jsps.2015.03.022>
10. Riederer MS, Requist BD, Payne KA, Way JD, Krebs MD. Injectable and microporous scaffold of densely-packed, growth factor-encapsulating chitosan microgels. *Carbohydr Polym* **2016**; 152: 792-801. <https://doi.org/10.1016/j.carbpol.2016.07.052>
11. Mathew AP, Uthaman S, Cho K-H, Cho C-S, Park I-K. Injectable hydrogels for delivering biotherapeutic molecules. *Int J Biol Macromol* **2018**; 110: 17-29. <https://doi.org/10.1016/j.ijbiomac.2017.11.113>
12. Luo Y, Kobler JB, Heaton JT, Jia X, Zeitels SM, Langer R. Injectable hyaluronic acid-dextran hydrogels and effects of implantation in ferret vocal fold. *J Biomed Mater Res Part B Appl Biomater* **2010**; 93: 386-93. <https://doi.org/10.1002/jbm.b.31593>
13. Rahbar Saadat Y, Hosseiniyan Khatibi SM, Ardalan M, Barzegari A, Zununi Vahed S. Molecular pathophysiology of acute kidney injury: The role of sirtuins and their interactions with other macromolecular players. *J Cell Physiol* **2020**; 236: 3257-74. <https://doi.org/10.1002/jcp.30084>
14. Rodriguez-Ruiz V, Salatti-Dorado JÁ, Barzegari A, Nicolas-Boluda A, Houaoui A, Caballo C, *et al.* Astaxanthin-loaded nanostructured lipid carriers for preservation of antioxidant activity. *Molecules* **2018**; 23: 2601. <https://doi.org/10.3390/molecules23102601>
15. Fathi M, Alami-Milani M, Geranmayeh MH, Barar J, Erfan-Niya H, Omid Y. Dual thermo- and pH-sensitive injectable hydrogels of chitosan/(poly (N-isopropylacrylamide-co-itaconic acid)) for doxorubicin delivery in breast cancer. *Int J Biol Macromol* **2019**; 128: 957-64. <https://doi.org/10.1016/j.ijbiomac.2019.01.122>
16. Amiraghoubi N, Pesyan NN, Fathi M, Omid Y. Injectable thermosensitive hybrid hydrogel containing graphene oxide and chitosan as dental pulp stem cells scaffold for bone tissue engineering. *Int J Biol Macromol* **2020**; 162: 1338-57. <https://doi.org/10.1016/j.ijbiomac.2020.06.138>
17. Fathi M, Majidi S, Zangabad PS, Barar J, Erfan-Niya H, Omid Y. Chitosan-based multifunctional nanomedicines and theranostics for targeted therapy of cancer. *Med Res Rev* **2018**; 38: 2110-36. <https://doi.org/10.1002/med.21506>
18. Pakzad Y, Fathi M, Omid Y, Mozafari M, Zamanian A. Synthesis and characterization of timolol maleate-loaded quaternized chitosan-based thermosensitive hydrogel: A transparent topical ocular delivery system for the treatment of glaucoma. *Int J Biol Macromol* **2020**; 159: 117-28. <https://doi.org/10.1016/j.ijbiomac.2020.04.274>
19. Cheng N-C, Lin W-J, Ling T-Y, Young T-H. Sustained release of adipose-derived stem cells by thermosensitive chitosan/gelatin hydrogel for therapeutic angiogenesis. *Acta Biomater* **2017**; 51: 258-67. <https://doi.org/10.1016/j.actbio.2017.01.060>
20. Barzegari A, Nouri M, Gueguen V, Saedi N, Pavon-Djavid G, Omid Y. Mitochondria-targeted antioxidant mito-TEMPO alleviate oxidative stress induced by antimycin A in human mesenchymal stem cells. *J Cell Physiol* **2020**; 235: 5628-36. <https://doi.org/10.1002/jcp.29495>
21. Barzegari A, Omid Y, Gueguen V, Meddahi-Pellé A, Letourneur D, Pavon-Djavid G. Nesting and fate of transplanted stem cells in hypoxic/ischemic injured tissues: The role of HIF1 $\alpha$ /sirtuins and downstream molecular interactions. *Biofactors* **2020**. <https://doi.org/10.1002/biof.1674>
22. Dang Q, Liu K, Zhang Z, Liu C, Liu X, Xin Y, *et al.* Fabrication and evaluation of thermosensitive chitosan/collagen/ $\alpha$ ,  $\beta$ -glycerophosphate hydrogels for tissue regeneration. *Carbohydr Polym* **2017**; 167: 145-57. <https://doi.org/10.1016/j.carbpol.2017.03.053>
23. Wu J, Su Z-G, Ma G-H. A thermo- and pH-sensitive hydrogel composed of quaternized chitosan/glycerophosphate. *Int J Pharm* **2006**; 315: 1-11. <https://doi.org/10.1016/j.ijpharm.2006.01.045>
24. Mohammadi S, Barzegari A, Dehnad A, Barar J, Omid Y. Astaxanthin protects mesenchymal stem cells from oxidative stress by direct scavenging of free radicals and modulation of

- cell signaling. *Chem Biol Interact* **2020**; 333: 109324. <https://doi.org/10.1016/j.cbi.2020.109324>
25. Rodriguez-Ruiz V, Barzegari A, Zuluaga M, Zunooni-Vahed S, Rahbar-Saadat Y, Letourneur D, et al. Potential of aqueous extract of saffron (*Crocus sativus* L.) in blocking the oxidative stress by modulation of signal transduction in human vascular endothelial cells. *J Funct Foods* **2016**; 26: 123-34. <https://doi.org/10.1016/j.jff.2016.07.003>
  26. Saadat YR, Saeidi N, Vahed SZ, Barzegari A, Barar J. An update to DNA ladder assay for apoptosis detection. *BioImpacts* **2015**; 5: 25. <https://doi.org/10.15171/bi.2015.01>
  27. Stec DE, Ishikawa K, Sacerdoti D, Abraham NG. The emerging role of heme oxygenase and its metabolites in the regulation of cardiovascular function. *Int J Hypertens* **2012**; 2012: 593530. <https://doi.org/10.1155/2012/593530>
  28. Zhang Z-h, Zhu W, Ren H-z, Zhao X, Wang S, Ma H-c, et al. Mesenchymal stem cells increase expression of heme oxygenase-1 leading to anti-inflammatory activity in treatment of acute liver failure. *Stem Cell Res Ther* **2017**; 8: 1-13. <https://doi.org/10.1186/s13287-017-0524-3>
  29. Hejazian SM, Khatibi SMH, Barzegari A, Pavon-Djavid G, Razi S, Hassannejhad S, et al. Nrf-2 as a therapeutic target in acute kidney injury. *Life Sci* **2021**; 264: 118581. <https://doi.org/10.1016/j.lfs.2020.118581>
  30. Ilghami R, Barzegari A, Mashayekhi MR, Letourneur D, Crepin M, Pavon-Djavid G. The conundrum of dietary antioxidants in cancer chemotherapy. *Nutr Rev* **2020**; 78: 65-76. <https://doi.org/10.1093/nutrit/nuz027>
  31. Friedenstein A, Piatetzky-Shapiro I, Petrakova K. Osteogenesis in transplants of bone marrow cells. *Development* **1966**; 16: 381-90. <https://doi.org/10.1242/dev.16.3.381>
  32. Pacelli S, Acosta F, Chakravarti AR, Samanta SG, Whitlow J, Modaresi S, et al. Nanodiamond-based injectable hydrogel for sustained growth factor release: preparation, characterization and in vitro analysis. *Acta Biomater* **2017**; 58: 479-91. <https://doi.org/10.1016/j.actbio.2017.05.026>
  33. Wei X, Yang X, Han Z-p, Qu F-f, Shao L, Shi Y-f. Mesenchymal stem cells: a new trend for cell therapy. *Acta Pharmacol Sin* **2013**; 34: 747-54. <https://doi.org/10.1038/aps.2013.50>
  34. da Silva Meirelles L, Fontes AM, Covas DT, Caplan AI. Mechanisms involved in the therapeutic properties of mesenchymal stem cells. *Cytokine Growth Factor Rev* **2009**; 20: 419-27. <https://doi.org/10.1016/j.cytogfr.2009.10.002>
  35. Harn H-J, Lin P-C, Su H-L, Chiou T-W, Lin S-Z. Pre-clinical studies and clinical application of adipose-derived stem cells. *J Neurosci Neuroeng* **2013**; 2: 14-28. <https://doi.org/10.1166/jnsne.2013.1031>
  36. Kinoshita Y, Maeda H. Recent developments of functional scaffolds for craniomaxillofacial bone tissue engineering applications. *Sci World J* **2013**; 2013: 863157. <https://doi.org/10.1155/2013/863157>
  37. Ma Q. Role of nrf2 in oxidative stress and toxicity. *Annu Rev Pharmacol Toxicol* **2013**; 53: 401-26. <https://doi.org/10.1146/annurev-pharmtox-011112-140320>